International Journal of Earth, Energy and Environmental Sciences
ISSN: 2517-942X
Vol:10, No:6, 2016

Discrete Element Modeling on Bearing Capacity Problems

N. Li, Y. M. Cheng

***Abstract*—**In this paper, the classical bearing capacity problem is re-considered from discrete element analysis. In the discrete element approach, the bearing capacity problem is considered from the elastic stage to plastic stage to rupture stage (large displacement). The bearing capacity failure mechanism of a strip footing on soil is investigated, and the influence of micro-parameters on the bearing capacity of soil is also observed. It is found that the distinct element method (DEM) gives very good visualized results, and basically coincides well with that derived by the classical methods.

***Keywords*—**Bearing capacity, distinct element method, failure mechanism, large displacement.

I. Introduction

BEARING capacity problem is always a main concern in geotechnical engineering. The problems of ultimate bearing capacity for shallow foundations with simple geometry have been solved by many investigators. These methods can be classified into the following four categories: (1) The limit equilibrium method [18]; [10]; (2) the method of characteristics [13]; [16]; [8]; [1]; [3]; (3) the upper-bound plastic limit analysis [14], [15]; [2]; [5]; [11], [12]; [17]; and (4) numerical methods based on either the finite-element technique or finite-difference method [7]; [6].

Besides the traditional classical method, for the problems with complicated geometry and loading conditions, the solutions are usually sought by finite element method. However, for granular material such as sand and gravel, its behaviour is significantly influenced by the particle features, which are difficult to model from the continuum mechanics. The failure mechanism and post-failure development are also important when analyzing the collapsing load of foundations. Therefore, the particle-based method provides an alternative to the aforementioned issue.

DEM initiated from [4] is now available as commercial program: PFC, particle flow code [9], is an alternate numerical method which is more suitable for large scale ground movement with separation, and it has the advantage in modeling the propagation of failure and the whole failure process after failure is triggered. It should be noted that there are very limited applications of the DEM for bearing capacity analysis, especially about the progressive failure mechanism of shallow foundations.

N. Li is the PhD student of Department of Civil and Environmental Engineering, Hong Kong Polytechnic University, Hong Kong (corresponding author: 852-6376-6459; fax: 852-2766-6042; e-mail: becksy.na@gmail.com).

Y. M. Cheng is the associate Professor of Department of Civil and Environmental Engineering, Hong Kong Polytechnic University, Hong Kong (e-mail: ceymchen@polyu.edu.hk).

The objective of this paper is to evaluate the bearing capacity problem by elasticity analysis, discrete element analysis, to provide failure mechanism from elastic stage to plastic stage and extend to large displacement stage. The large scale failure mechanism and movement of soil on the bearing capacity of a strip footing is further investigated, and the influence of micro-parameters on the bearing capacity of soil is also observed. A numerical solution is established by using a distinct-element-based procedure of the software PFC2D (particle flow code in two-dimension). The numerical results obtained are then compared with the classical methods of Prandtl [13].

II. Bearing Capacity Theory

In general, the development of bearing capacity theory can be concluded as follows: application of limit equilibrium methods was first done by Prandtl on the punching of thick masses of metal. Prandtl's methods were then adapted by Terzaghi [18] to bearing capacity failure of shallow foundations. Vesic [19] and others improved on Terzaghi's original theory and added other factors for a more complete analysis.

Prandtl [13] proposed the strip footing's ultimate bearing capacity for a frictional-cohesive material loaded by a uniformly distributed pressure q, and applying the principle of superposition, the formula can be written as:

$$q_u = cN_c + qN_q \tag{1}$$

where $N_c = (N_q - 1)\cot\phi$, $N_q = e^{\pi\tan\phi}\tan^2\left(45+\frac{\phi}{2}\right)$

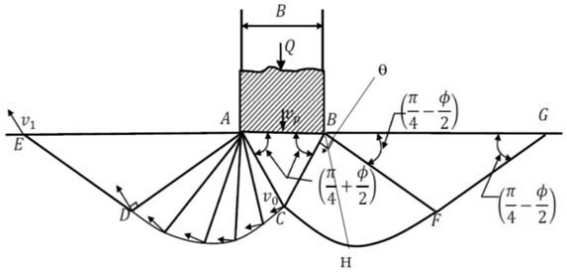

Fig. 1 Prandtl Mechanism

Prandtl considered the bearing capacity of a weightless soil. Prandtl mechanism is illustrated in Fig. 1. When estimating the influence of γ on bearing capacity, $N_\gamma = 2(N_q+1)\tan\phi$ is used

by Vesic and adopted in GEO Guide in Hong Kong, and it is also used in this study to combine with Prandtl's formula in the comparison of the subsequent section.

III. DEM Model Generation

In the numerical study by DEM based particle flow analysis, the width B of the rigid footing is set as 400 mm. Since the problem is symmetric, only half of the problem domain is considered, so that the footing width in model is 200 mm. The half-domain has a depth of 3000 mm and extends 5800 mm beyond the edge of the footing, which is large enough to neglect the ''boundary influence'' on the estimation of the collapse load as well as for the prediction of failure mechanism (shown in Fig. 2). A loading pattern of strain control/velocity control is applied. The uniform loading was simulated by applying a vertical velocity of 0.01 mm/s on the footing.

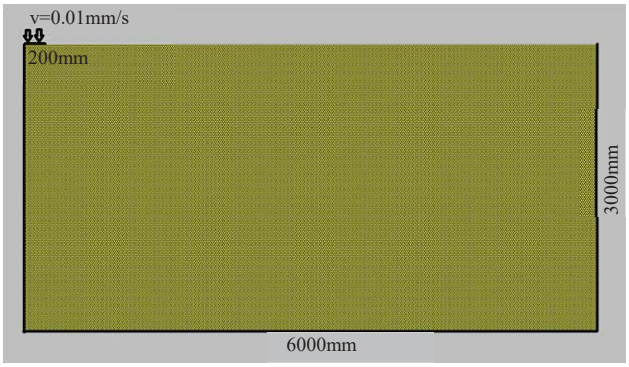

Fig. 2 PFC Model for the simulation

The micro-properties of the sandy soil as shown in Table I are determined by varying the micro-properties until the macro-properties obtained numerically match with the experimental results (angle of repose and stress-strain relation).

TABLE I
Microscopic Parameters of the Sands for Particle Flow Analysis

Microscopic Parameters	Value (units)
Density (kg/m^3)	2650
Normal and shear stiffness (N/m^2)	1 x 10^7
Frictional coefficient of particle	0, 0.577; 0.700; 0.839
Diameter of particle (mm)	0.02; 0.06; 0.1
Contact Bond - Normal Strength (N)	0; 1000; 5000; 10000
Contact Bond - Shear Strength (N)	0; 1000; 5000; 10000

According to the experiment by Vesic [19], the failure mode types for a shallow foundation depends on the relative-density and the depth ratio D/B. General shear failure occurs at higher relative density while punching shear failure occurs at lower relative density. Therefore, two extreme conditions which are the very densely-packed and loosely-packed soil particles were studied. The porosities of very densely-packed and loosely-packed particles are 0.0932 and 0.2144 respectively, and two types of particle packing in numerical study are illustrated in Fig. 3.

IV. Elasticity Analysis of Bearing Capacity of a Strip Footing on Sandy Soils

Settlement is generally defined as the downward movement of soil at a point, which is essential to be considered in civil engineering. The settlement of a foundation must be controlled in order to satisfy the serviceability limit state (SLS) in the foundation design. In Hong Kong, the new maximum settlement for a foundation structure is limited to 30 mm. The elastic settlement at a point is calculated by using the elastic solution:

$$\Delta H = I_f q_0 B' \frac{1-\mu^2}{E_s}\left(I_1 + \frac{1-2\mu}{1-\mu} I_2\right) \quad (2)$$

where I_f = Depth Factor, $q_0 = q_{net} = q_{total} - \gamma D$, B'= effective width, μ = Poisson's ratio and I_1、I_2 are influence factor of foundation geometry.

The total foundation settlement is equal to the sum of elastic settlement and consolidation settlement. Since the water table is not considered, the consolidation settlement is ignored. Therefore, the total foundation settlement equal to the elastic settlement can be calculated according to (2). Consider the settlement ranging from 0 to 20 mm. $\frac{D}{B_{min}} = \frac{0}{400} = 0$ and $\frac{D}{B_{max}} = \frac{20}{400} = 0.05$, which are comparably small. Since square footing is used, $\frac{L}{B} = \frac{840}{840} = 1$, using Fig. 4, we can find that the depth factor I_f changes from 1 to 0.95 for varying depth ratio, which is not a significant change. Therefore, the depth factor vary I_f can be approximately treated as a constant. Settlement of 20 mm is very small comparing to the 3000 mm depth of soil, therefore I_1 and I_2 can be taken as constant. Yield point is not reached for the first 20 mm settlement and the Young's Modulus E_s can also be assumed to be constant. The effective width B' and the Poisson's ratio μ are always constant as they are the material properties. Therefore, theoretically, the settlement ΔH is directly proportional to the uniform loading q_0 on the foundation.

Next to check out the numerical result, the value of the vertical stress σ_{yy} for the first 60 mm settlement were recorded in the DEM simulation in order to investigate its development during the serviceability limit state, and the data for load/settlement relation have been further plotted in Fig. 5 with different soil friction angles. Consider the first 20 mm settlement in Fig. 5, the value of σ_{yy} for ϕ =0°, 30°, 35° and 40° were the same and the corresponding curve is linear. Results from PFC indicate that the settlement is directly proportional to the vertical stress developed during the elastic stage before reaching the yield point. Thus, the theoretical elasticity phenomenon coincides with the results obtained by using PFC. The value of σ_{yy} for ϕ =30°, 35° and 40° started to be different when the settlement exceeds 20 mm. At this moment, the soil starts to yield in regarding to its soil properties (friction angle and cohesion). The deformation is no longer elastic then.

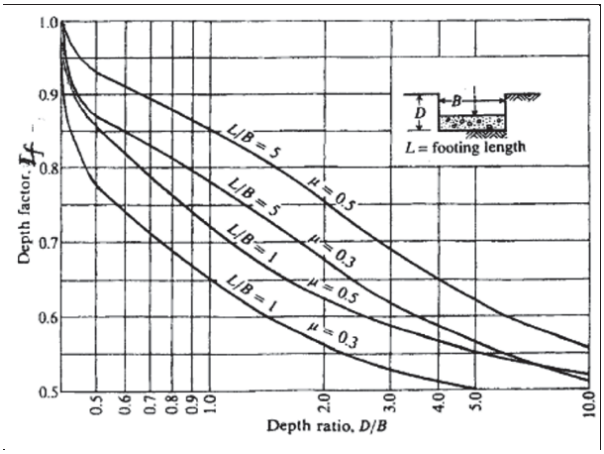

Fig. 4 Variation of depth factor If with depth ratio D/B

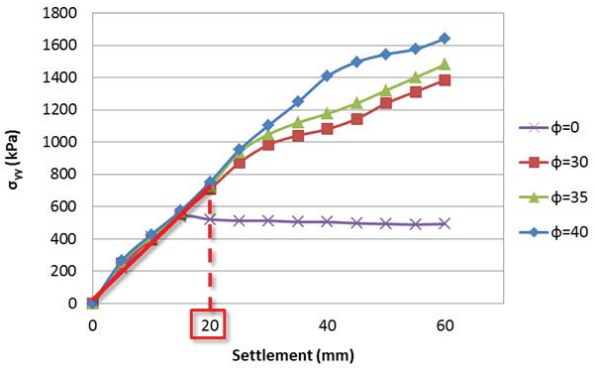

Fig. 5 Variation of vertical stress with different settlement

V. Failure Pattern of Bearing Capacity Problem under Large Displacement Simulation

A. Punching Shear Failure of Loosely Packed Soil

A special case of foundation problem with loosely-packed particles has also been performed. As shown Fig. 6, it is noticed that considerable vertical displacement takes place in the vertical direction along the edges of the foundation, and the settlement is continuously increasing. Failure surface does not extend beyond the zone right beneath the foundation, as noticed in Fig. 6 (d). It is found that punching shear failure is formed in the numerical analysis which is common in fairly loose sand or soft clay. This mode of failure occurs also in soil of low compressibility.

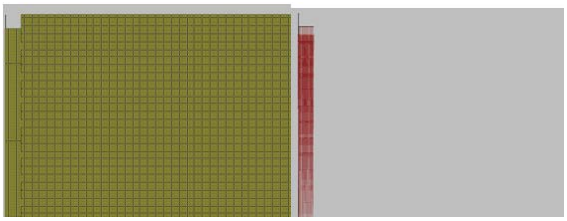

(a) (b)

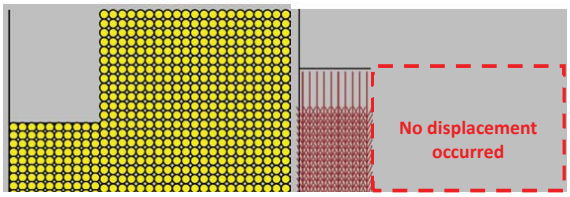

(c) (d)

Fig. 6 Punching shear failure (contact bond=0, ϕ =35o, loose) (a) Model under uniform loading, (b) Displacement vectors of punching shear failure (c) Close-up view for punching shear failure and (d) Close-up view of punching shear failure

B. General Shear Failure Mechanism of Densely Packed Soil

Densely packed soil foundation is studied to investigate the general shear failure mechanism under uniform loading. The progressive failure progress is illustrated as follows in Fig. 7, for the soil with contact bond strength of 5kN.

The loading footing induces a downward movement of underlying soil particles. Firstly, there is small disturbed area under loading footing, then the affected area is extended. We can clearly observe two zones, the formation of a clear boundary for Zone I: Active Rankine Zone is noticed in Fig. 7 (c). Soil particles underneath the foundation move further to the bottom right and Zone II: Prandtl Zone is developed. Upheaval at ground surface further develops away from the edge of footing. Soils move further to the upper right, but unit weight of soils (surcharge) resists the shear slipping. Next, Plasctic Zone III: Rankine's Passive Zone is formed in Fig. 7 (d). Soils within the Passive Rankine Zone are pushed by the ones from Zone II and start to move upward causing upheaval. Then, the shear band boundary of Zone II is produced, and the primary shear failure surface penetrated through the plastic zone when settlement reaches 100mm as shown in Fig. 7 (e). Soil particles far away from the footing are affected by the shear slipping and the primary plastic failure zones further develop. Gradually, a secondary shear failure surface is formed and upheaving continuous to grow, as noticed in Fig. 7 (f), also a typical view of failure zones with shear failure surface is pinted out in Fig. 7 (f). Further upheaval and deep disturbance to soils occur due to the excessive settlement in Fig. 7 (g), at this stage, the foundation is no longer a shallow foundation problem since the depth of footing is equal to the width of footing, and now it becomes a deep foundation problem. Moreover, multiple failure zones are viewed as water ripples in Figs. 7 (g) & (h), which represent the transformation of plastic zones from disturbance area to the surroundings. Eventually, the displacement vectors form an anti-clockwise circular loop, and 650mm settlement is generated after 65000 time-steps have been executed, see as Fig. 7 (h). From this typical failure progress of shallow foundation, DEM gives really good visualized results, as shown in Fig. 7. These obtained failure patterns coincide fairly well with that of plastic theory by Prandtl mechanism (Fig. 1). Among all, the failure patterns of active and transition zone are similar but soil particles with higher friction angle have larger passive zone, demonstrated in Fig. 9.

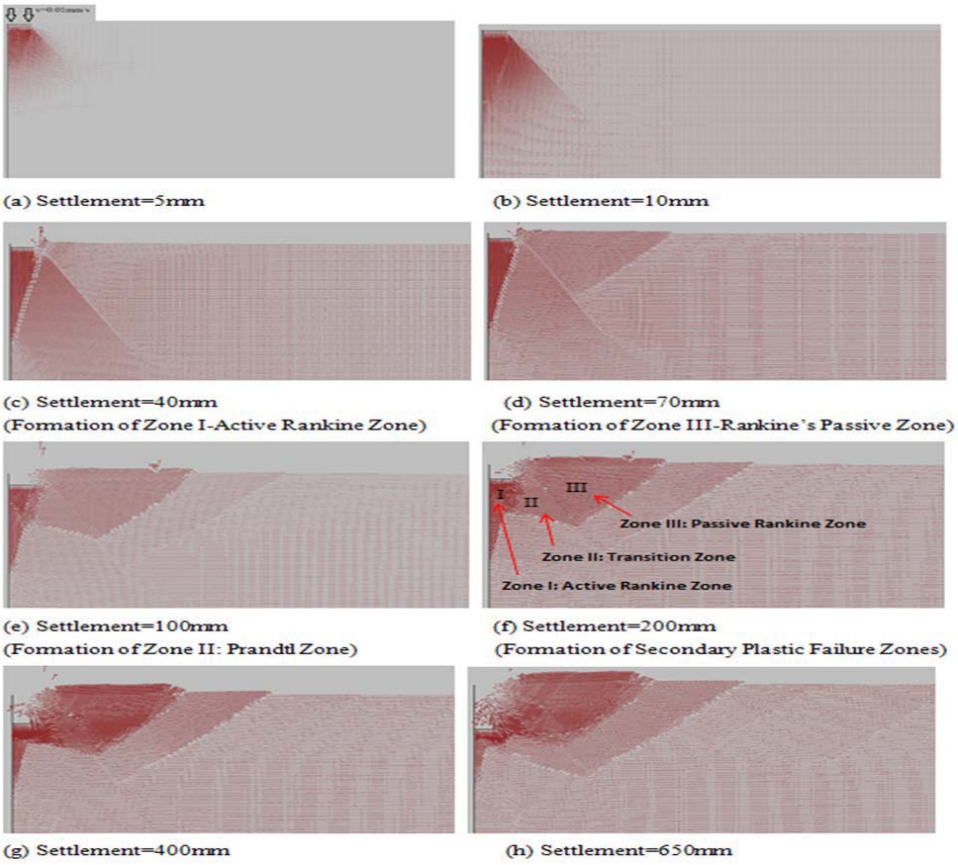

Fig. 7 Failure progress of densely packed soil foundation (contact bond=5kN, ϕ =35^o)

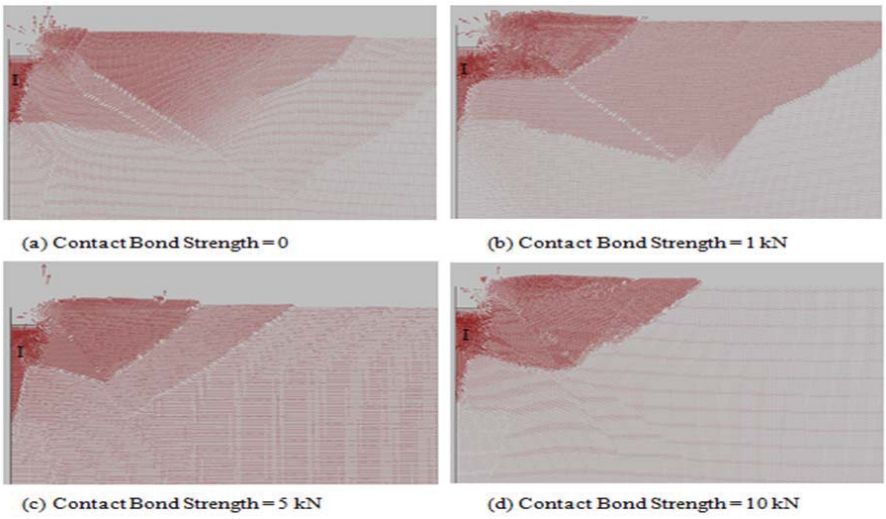

Fig. 8 Shear failure mode of a strip foundation under ultimate bearing capacity with different contact bond strength of sandy soil (friction angle ϕ = 35^o)

C. Influence of Bond Strength

Four values of contact bond strength, 0, 1, 5, 10 kN are considered for soil with friction angle ϕ = 35^o, to study for the influence of bond strength to the failure mechanism, the shear failure modes for each bond strength under same settlement are represented in displacement vector in Fig. 8. When considering the area of Active Rankine Zone (Zone I), failure pattern is quite similar. However, the area of soil disturbance zone decreases from bond strength = 0 to 5kN, which demonstrates larger shear resistance from larger contact bonding between

particles, and the particle movement inside the disturbance zone grows larger to eliminate the energy transferred from loading footing, noticing from the most obviously highlighted displacement vector in Fig. 8 (d).

D.Influence of Friction Angle

Four values of friction angles, 0°, 30°, 35°, 40° are considered for soil with contact bond strength = 5 kN, to study for the influence of friction angle to the failure mechanism. The shear failure modes for each friction angle under same settlement are represented in displacement vector in Fig. 9. It is found that the shape of the failure depends mostly on the friction angle. Angle of Zone I, ψ_a, differs from Figs. 9 (a) to (d), and the area of Zone I grows larger with steeper triangle following with growing disturbance area (plastic failure zone), so that failure patterns among these four cases are different. Thus, friction angle influences more than bond strength to the shear failure mode of foundation, comparing Fig. 8 with Fig. 9, which illustrates the DEM results are consistent with the classical solution where ψ_a equals to $45^o + \frac{\phi}{2}$. Meanwhile, with the increasing soil friction angle, the disturbed area becomes larger and larger, also observed from Fig. 9.

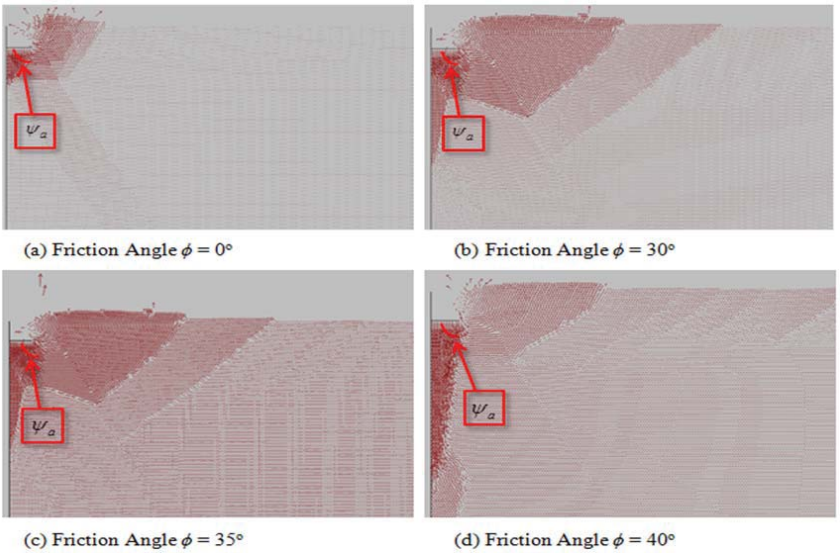

Fig. 9 Shear failure mode of a strip foundation under ultimate bearing capacity with different friction angles of sandy soil (contact bond strength = 5 kN)

VI. Discussions

A. Discussion of the Load-Settlement Relation

The load-settlement relation with the variation of soil friction angles, obtained from simulation, is plotted in Fig. 10. When ϕ = 35°, the ultimate bearing capacity (vertical stress σ_{yy}) is around 2400 kPa, then stress is increased by increasing the friction angle. When friction angle =40°, the q_{ult} reaches its largest value, which is 3200 kPa. Inter-particle bonds are mobilized in the first stage of ascent curve till it increases to the peak resistance, then some inter-particle bonds are broken, beavering as curves drop, but microstructure is still randomly oriented in the first beginning, where mostly frictional resistance still work. Then, ultimate bearing capacity becomes steady, following with large deformation in the disturbance area, producing an aligned microstructure, eventually soil foundation obtains its residual strength for around 1000 kPa. As shown in Fig. 10, the curve of numerical results is similar to that of the classical theory, which can be explained that initial interlocking effect between dense sand particles has been progressively overcome during compression, and shear dilatancy effect for dense sand occurs followed with volume change and porosity increase. The phenomenon is illustrated in Fig. 11. It can be concluded that as footing settlement takes place in the very beginning, compression to soil particle is induced to overcome the interlocking effect, resulting in soil mass volume increase as well as porosity increase, followed by slipping (shear failure), volume expansion and upheaval on ground surface. From the variation of soil porosity as shown in Figs. 11 (c) and (d), the trend of porosity change looks similar between the numerical and laboratory results.

B. Discussion of Ultimate Bearing Capacity between Basic Limit Equilibrium Formulations & DEM Simulation

Fig. 12 shows the variation of ultimate bearing capacity with friction angle/bond strength obtained by DEM based particle flow analysis. Fig. 13 shows the variation of the ultimate bearing capacity with friction angle/cohesion obtained by Vesic Equation. Generally, they are of the same tendency. The ultimate bearing capacity q_{ult} increases with the friction angle. Except the result obtained from ϕ = 40° with contact bond strength = 0, it is found that the ultimate bearing capacity q_{ult} also increases with the contact bond strength (which is of similar idea to cohesion). Therefore, DEM shows that the ultimate bearing capacity q_{ult} of soil particles increases with both friction angle and bond strength (cohesion), but as

mentioned above, friction angle influences the bearing capacity more than the bond strength, and DEM numerical results coincide with the results from classical Limit Equilibrium Method.

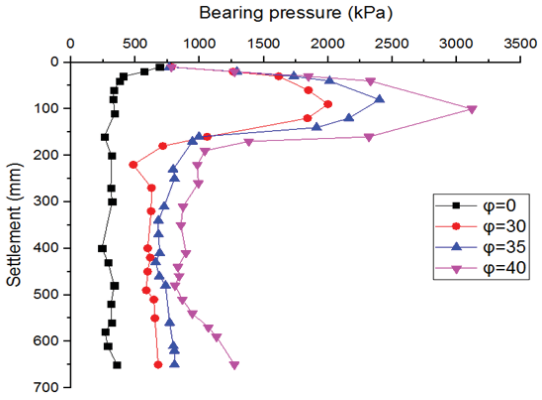

Fig. 10 Load-settlement curves with different friction angles for bond strength = 10kN

VII. Conclusion

In this study, elasticity analysis and discrete element analysis are used to study the bearing capacity problem of a shallow foundation. For the elasticity analysis, the general behaviors of soil particles analyzed by Discrete Element Method are consistent with that derived by the theoretical elasticity method. For the ultimate limit state, failure pattern of bearing capacity problem under large displacement simulation is emphatically studied by DEM. Densely packed soil foundation is considered to investigate the general shear failure mechanism. The progressive failure progress is studied and concluded as follows: as the uniform loading is applied to footing acting on soil, firstly there is small disturbed area under footing, then plastic area is extended showing clear view of Plastic Zone I and Zone II, and finally Zone III appears. Next, shear failure surface becomes continuous, following with upheaval in ground surface. As settlement keep increasing, plastic zones extend to the surrounding area, so secondary failure surface occurs and multiple failure zones show up, and the plastic failure transfers to a larger disturbed area followed with the further upheaval.

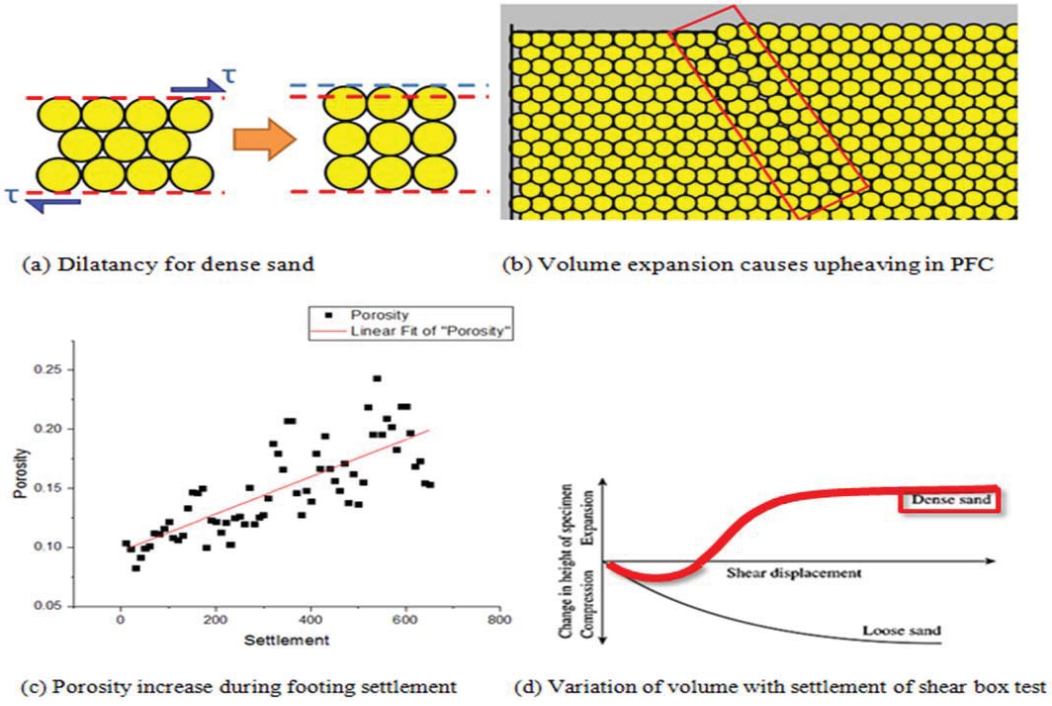

Fig. 11 Phenomenon of loading on shallow foundation for dense sands

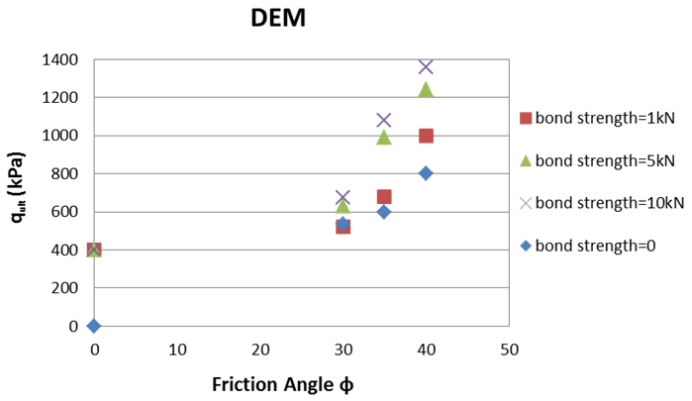

Fig. 12 Variation of q_{ult} with friction angle/bond strength obtained by DEM

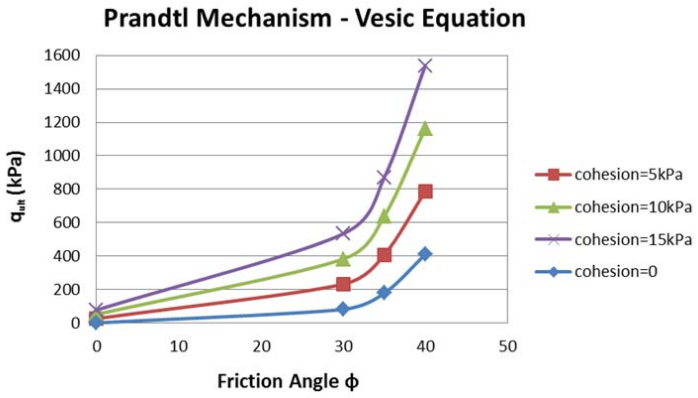

Fig. 13 Variation of q_{ult} with friction angle/bond strength using Prandtl Mechanism

It is also found that punching shear failure occurred which is common in fairly loose sand or soft clay. This mode of failure occurs also in soil of low compressibility. Friction angle influences more than the bond strength for the shear failure of foundation and the bearing capacity. Moreover, the phenomenon of uniform loading on shallow foundation for dense sands can be concluded as the settlement of footing takes place in the very beginning, inducing compression to soil particles to overcome the interlocking effect, followed by volume increase and porosity increase (shear dilatancy effect) of soil mass, resulting in slipping (shear failure), volume expansion of soil and upheaval on ground surface.

Above all, DEM gives very good visualized results, and basically coincides well with that derived by the classical understanding. Therefore, DEM seems to be a more appropriate method to analyze the behaviors of discontinuities. It can provide additional insights into many geotechnical problems which are not possible with other methods.

Acknowledgment

The authors would like to thanks to the support from the Hong Kong Polytechnic University through project RTMJ and the Research Grant Council project PolyU 5128/13E.

References

[1] M.D. Bolton and C.K. Lau, "Vertical bearing capacity factors for circular and strip footings on Mohr-Coulomb soil". *Canadian Geotechnical Journal*, 30(4):1024–1033, 1993.
[2] W.F. Chen, *Limit analysis and soil plasticity*. Elsevier, New York, 1975.
[3] Y.M. Cheng and S.K. Au, "Slip line solution of bearing capacity problems with inclined ground". *Canadian Geotechnical Journal*, vol.42, 1232-1241, 2005.
[4] P.A. Cundall and O.D.L.Strack, "A discrete model for granular assemblies". *Geotechnique*, 29(1):47-65, 1979.
[5] A. Drescher and E.Detournay, "Limit load in translational failure mechanisms for associative and non-associative materials". *Geotechnique*, London, 43(3), 443–456, 1993.
[6] S. Frydman and H.J. Burd, "Numerical studies of bearing-capacity factor N-gamma". *J. Geotech. and Geoenvir. Engrg., ASCE*, 123(1): 20-29, 1997.
[7] D.V. Griffiths, "Computation of Bearing Capacity Factors Using Finite-Elements". *Geotechnique*, 32(3): 195-202, 1982.
[8] B.J. Hansen, "A general formula for bearing capacity". *Bull. Dan. Geotech. Inst.*, 11: 38–46, 1961.
[9] Itasca, *PFC2D 3.10 Particle Flow Code in Two Dimensions, Theory and Background volume* (Third ed.). Minneapolis, Minnesota, 2004.
[10] G.G. Meyerhof, "The ultimate bearing capacity of foundations". *Geotechnique*, 2: 301-332, 1951.
[11] R.L. Michalowski, "Slope stability analysis: A kinematical approach". *Geotechnique*, London, 45(2), 283–293, 1995.
[12] R.L. Michalowski, "An estimate of the influence of soil weight on bearing capacity using limit analysis". *Soils and Found.*, Tokyo,37(4), 57–64, 1997.
[13] L. Prandtl, "Über die Härte plastischer Körper". Göttingen Nachr. *Math. Phys. K1.*, 12, 74-85, 1920.

[14] R.T. Shield, "Plastic potential theory and the Prandtl bearing capacity solution". *J. Appl. Mech.*, 21, 193–194, 1954a.
[15] R.T. Shield, "Stress and velocity fields in soil mechanics". *J. Math. Phys.*, 33(2), 144–156, 1954b.
[16] V.V. Sokolovskii, *Statics of Granular Media*, Pergamon Press, 1965.
[17] A.H. Soubra, "Upper-bound solutions for bearing capacity of foundations". *J. Geotech. and Geoenvir. Engrg., ASCE*, 125(1), 59–68, 1999.
[18] K. Terzaghi, *Theoretical soil mechanics*. New York: Willey, 1943.
[19] A.S. Vesic, "Analysis of ultimate loads of shallow foundations". J. Soil Mech. Found. Div., ASCE 99, No. SM1, 45–73, 1973.